

Three-D Investigation of Thick Single Lap Bolted Joint

Florin Iancu,
Research Assistant
Mechanical Engineering Dept., Michigan State University, East Lansing, MI, 48824, USA

Xu Ding
Research Assistant
Mechanical Engineering Dept., Michigan State University, East Lansing, MI, 48824, USA

Gary L. Cloud, P.E.
Professor
Mechanical Engineering Dept., Michigan State University, East Lansing, MI, 48824, USA

Basavaraju B. Raju
Senior Research Engineer
US Army Tank Automotive Command, Warren, MI, 48397, USA

ABSTRACT

Stresses in single-lap bolted joints of thick plates are complex and difficult to analyze. Previous studies involving stresses through the thickness of bolted joints have been limited to Finite Element Method (FEM) simulations and have been implemented only for the joining of relatively thin plates.

This paper reports on several experimental and numerical analyses that were conducted to analyze the stress distribution inside thick bolted plates along the bearing plane normal to the plate surface. Experimental analysis was conducted via embedded-polariscope photoelasticity and embedded resistance strain gages. The FEM analysis was performed with the Abaqus commercial code using material properties and other data obtained experimentally as input. Experimental and numerical results agreed reasonably well, and are believed to depict the behavior of the joint under load well enough to assist in development of improved joint design.

Having established confidence in the numerical model, two alternative designs were analyzed with the objective of decreasing the value of the maximum stress. The first plate presented a steel bushing that lined the hole, and the maximum stress in that case was decreased by 50%. The second design had the edges of the hole chamfered at a 45-degree angle. This design did not exhibit a decrease in the maximum stress, but it did show an advantageous change in the position of the maximum stress.

INTRODUCTION

Bolt fastening is the most widely spread method of Joining because it is a non-permanent joint, it is easy to set up in a variety of conditions, it facilitates disassembly and repair, and, most of the time, it does not require manufacturing of special parts, which makes it less expensive. The problem of fastening composite materials using bolted joints is a very troublesome, because stress concentrations develop around the holes, severely reducing the strength and fatigue life of the structure. To utilize the full potential of Fiber Reinforced Polymers (FRP) in structural elements, appropriate methods for stress analysis must be developed.

Camanho and Matthews (1997) [1] summarized the previous work in predicting the failure of bolted joint composite in their review paper. The conclusion was that by taking the composite to the ultimate load, very little information could be extracted. Most of the studies on mechanically fastened joints have focused on failure tests of the structures [1, 2, 3, 4, 5, 6, 7]. Relatively few studies deal with 3-D stress analysis of bolted joints. Among the first finite element solutions created for studying contact stresses were the ones of Chen, Lee and Yeh, in 1995 [8]. They were based on an incremental variational principle and the

Report Documentation Page

Form Approved
OMB No. 0704-0188

Public reporting burden for the collection of information is estimated to average 1 hour per response, including the time for reviewing instructions, searching existing data sources, gathering and maintaining the data needed, and completing and reviewing the collection of information. Send comments regarding this burden estimate or any other aspect of this collection of information, including suggestions for reducing this burden, to Washington Headquarters Services, Directorate for Information Operations and Reports, 1215 Jefferson Davis Highway, Suite 1204, Arlington VA 22202-4302. Respondents should be aware that notwithstanding any other provision of law, no person shall be subject to a penalty for failing to comply with a collection of information if it does not display a currently valid OMB control number.

| | | | | | |
|--|--|---|---|----------------------------------|---------------------------------|
| 1. REPORT DATE 14 JUN 2004 | 2. REPORT TYPE Journal Article | 3. DATES COVERED 16-03-2004 to 27-05-2004 | | | |
| 4. TITLE AND SUBTITLE Three-D Investigation of Thick Single Lap Bolted Joint | | 5a. CONTRACT NUMBER | | | |
| | | 5b. GRANT NUMBER | | | |
| | | 5c. PROGRAM ELEMENT NUMBER | | | |
| 6. AUTHOR(S) Florin FIancu; Xu Ding; Gary Cloud,; Basavaraju Raju | | 5d. PROJECT NUMBER | | | |
| | | 5e. TASK NUMBER | | | |
| | | 5f. WORK UNIT NUMBER | | | |
| 7. PERFORMING ORGANIZATION NAME(S) AND ADDRESS(ES) Mechanical Engineering Dept.,Michigan State University,428 S.Shaw Lane, Rm. 2555,East Lansing,Mi,48824 | | 8. PERFORMING ORGANIZATION REPORT NUMBER ; #14181 | | | |
| 9. SPONSORING/MONITORING AGENCY NAME(S) AND ADDRESS(ES) U.S. Army TARDEC, 6501 East Eleven Mile Rd, Warren, Mi, 48397-5000 | | 10. SPONSOR/MONITOR'S ACRONYM(S) TARDEC | | | |
| | | 11. SPONSOR/MONITOR'S REPORT NUMBER(S) #14181 | | | |
| 12. DISTRIBUTION/AVAILABILITY STATEMENT Approved for public release; distribution unlimited | | | | | |
| 13. SUPPLEMENTARY NOTES | | | | | |
| 14. ABSTRACT Stresses in single-lap bolted joints of thick plates are complex and difficult to analyze. Previous studies involving stresses through the thickness of bolted joints have been limited to Finite Element Method (FEM) simulations and have been implemented only for the joining of relatively thin plates. This paper reports on several experimental and numerical analyses that were conducted to analyze the stress distribution inside thick bolted plates along the bearing plane normal to the plate surface. Experimental analysis was conducted via embedded-polariscope photoelasticity and embedded resistance strain gages. The FEM analysis was performed with the Abaqus commercial code using material properties and other data obtained experimentally as input. Experimental and numerical results agreed reasonably well, and are believed to depict the behavior of the joint under load well enough to assist in development of improved joint design. Having established confidence in the numerical model, two alternative designs were analyzed with the objective of decreasing the value of the maximum stress. The first plate presented a steel bushing that lined the hole, and the maximum stress in that case was decreased by 50%. The second design had the edges of the hole chamfered at a 45-degree angle. This design did not exhibit a decrease in the maximum stress, but it did show an advantageous change in the position of the maximum stress. | | | | | |
| 15. SUBJECT TERMS | | | | | |
| 16. SECURITY CLASSIFICATION OF: | | | 17. LIMITATION OF ABSTRACT Public Release | 18. NUMBER OF PAGES 10 | 19a. NAME OF RESPONSIBLE PERSON |
| a. REPORT unclassified | b. ABSTRACT unclassified | c. THIS PAGE unclassified | | | |

transformation matrix derived from three-dimensional contact kinematics conditions. The model took into account the effects of friction, clearance, bolt elasticity, stacking sequence and contact tractions around the bolted joint.

Another finite element analysis for laminate composite joints was developed by Barbero, Luciano and Sacco [9]. In their paper, a contact/friction iso-parametric finite element for the analysis of connections between laminated composite plates is presented. A three-dimensional finite element model of bolted composite joints was developed by Ireman [10] to determine the non-uniform stress through the thickness of the composite laminates in the vicinity of a bolt hole. The numerical model results were compared with experimental results obtained by strain gage measurement.

Because of the complexity and difficulty of stress analysis on thick single-lap bolted joints, as described above, all studies on stress analysis through the thickness of bolted joints carried out so far have been limited to Finite Element simulations and only for thin plate joints. As well, experimental results are highly desired to understand, more in detail, the real stress distribution in the through-thickness direction of bolted joints. No study on stress fields of thick single-lap bolted joints was found.

RESEARCH OBJECTIVES

A thick single-lap bolted joint of an epoxy plate with an aluminum one were investigated by experiments and finite element analysis. The numerical results were correlated with the experimental ones, which were obtained through two test methods: embedded photoelasticity and strain gage measurements.

The three methods used in this study were chosen for a number of reasons. The embedded photoelasticity method was used for having the advantage of being the only experimental method able to provide directly the values of stresses in the through-thickness direction. The disadvantage of using an embedded polariscope is that the Tardy goniometric compensation method can not be used for fringe fraction measurements. Because of this, the results obtained by experiment have a significant error margin. Some strain gages were utilized because of their accurate response. The relation between the strain measured by strain gages and the stress measured by photoelasticity can be easily verified.

The finite element analysis provides results much cheaper, faster and flexibly than experiments. For creating a reliable FEA model, first, a model that can be verified experimentally has to be created. Then, improvements of that model can be simulated, and qualitative as well as quantitative results can be obtained. The most difficult problem when dealing with finite element modeling of a joint resides in the necessity of creating contact surfaces. The parameters of the contact surface will greatly affect the final result. The problem becomes even more complicated when non-isotropic materials are involved. The second problem when trying to create a FEA model of the single-lap joint is simulating the clamping force that is imposed by the torque applied to the bolt and nut.

The load cases studied are as follows: (1) pin connected - the two plates are joined by a pin and an extension force is applied on the end of one plate, while the other plate is fixed on the direction of the extension; (2) the pin was replaced by a bolt and the joint was studied for several magnitudes of torque applied to the bolt-nut pair including finger tightening (approx. 3 in-lbs of torque), 25 in-lbs torque and 40 in-lbs torque.

EXPERIMENTAL METHODS

Two methods were implemented: the embedded polariscope photoelasticity method was used to determine the shear stress distribution in the bearing plane, and resistance strain gages were employed for measuring strain in the same plane.

1. Manufacturing of specimen.

In our case, the polarizer, the analyzer and the quarter wave plates were embedded into the specimen, as shown in Figure 1. The polarizer and the retarding film were cut from commercially available sheet of Polaroid filter medium, type CP -01P (made by International Polarizer, Inc.). The quarter wave plates have the role of converting the linear polarized light emerging from the polarizer into circularly polarized light. The circular polarization eliminates isoclinics (loci of points of constant inclination of the principal axes of refraction)

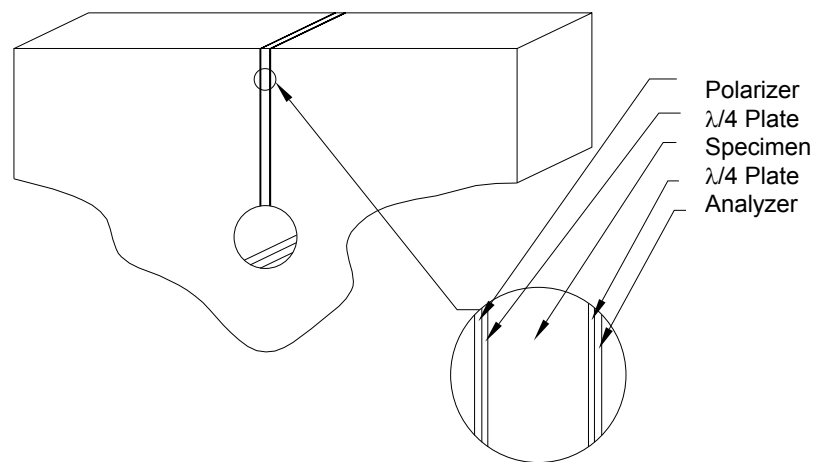


Figure 1. Embedded polariscope in a birefringent material plate.

A 4 by 8 inch piece was cut out from a commercial photoelastic sheet (PSM-9), manufactured by Photoelastic Division of Measurements Group, Inc. The material has the following material properties: $E = 4.78 \text{ e5psi}$, $\nu = 0.38$, and the material has the great advantage of being a birefringent material. A hole of $15/32$ inches in diameter was drilled at 1.5 inches from the short side and 2 inches from the long side as in Figure 2. From the hole to the short side, a 0.185 inches slice or slat was removed. Three strain gages were attached to the slice as in Figure 3.



Figure 2. Initial stage in the construction of the specimen.

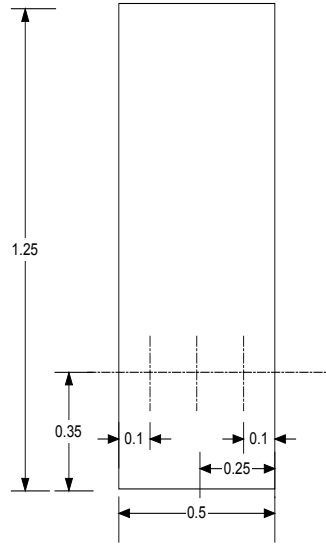


Figure 3. Strain gages attached to the removed slice



Next, a polarizer and retarded plates were glued on both sides of the slice to form a light field polariscope. See Figure 4. After all these operations, the slice was glued back into its original place inside the plate and the bolt hole was reamed to 0.5 inches as shown in Figure 5.



Figure 4. The final form of the specimen.

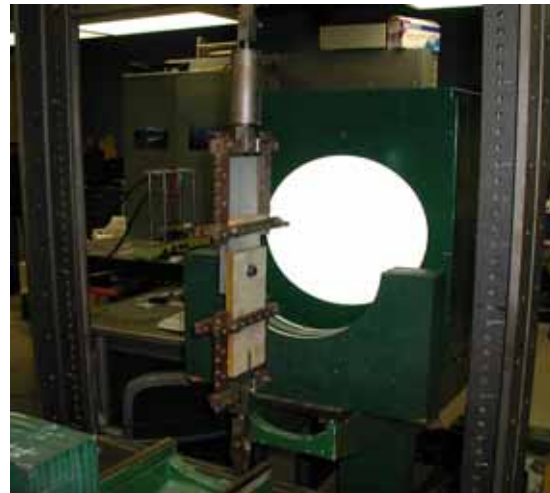


Figure 5. Loading frame.

2. Loading conditions

The loading frame can be seen in Figure 5.

Both plates are $8 \times 4 \times .5$ inches. The investigated plate was made as described in section 1. The supporting plate is made of aluminum, 2024-T4, with the following material properties: $E = 1.01 \text{ e7psi}$, $\nu = 0.34$. During tests, photoelasticity fringe patterns were recorded by a COHU CCD camera and the strain readings from strain gages were obtained by commercial strain indicators.

FINITE ELEMENT ANALYSIS

The numerical study of the single lap joint was done using the explicit finite element code ABAQUS 6.2 [11]. The preprocessor used to build the finite element model was HyperMesh 5.0 [12], and the postprocessor used to view the results was ABAQUS/Viewer 6.3-1. Several finite element models were created in order to study the two types of joints: pin connected and bolt connected. A typical mesh of the bolt connected joint is shown in Figure 6.

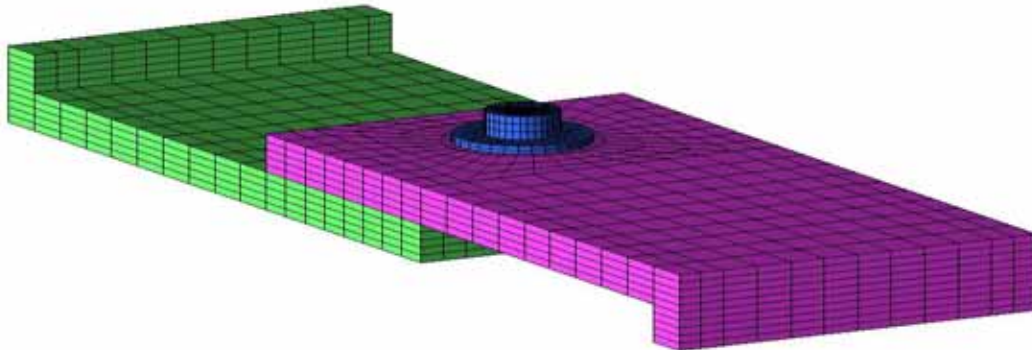


Figure 6. Typical mesh of a single lap bolted joint of two plates.

The mesh is divided into two regions: a square corresponding to the overlap area with a finer mesh surrounding the bolt hole and a rectangle with a coarser mesh. The plates have an offset part at the ends so the loading conditions can be uniaxial. The square is in turn divided into two sub-parts: a cylindrical part under the washers and the rest of the square. Thirty-two elements were used around the hole. The same number of elements was used to model the circumference of the bolt and bolt head. All the elements used for modeling the geometry were C3D8I, eight-node, solid elements.

The bolt, bolt head and washer were modeled as a single object to limit the number of contact surfaces in the model. The nut was modeled together with the second washer and a contact pair was created between the inside of the washer and the outside of the bolt. A high friction coefficient was applied to these surfaces, in order to simulate the effect of the thread. Figure 7 shows the nut-washer component and the whole fastening assembly. The model was based on idealization of the fastening system [13]. The torque applied to the bolt and nut was converted into a compressive load applied to the bolt-head and nut (see Figure 8).

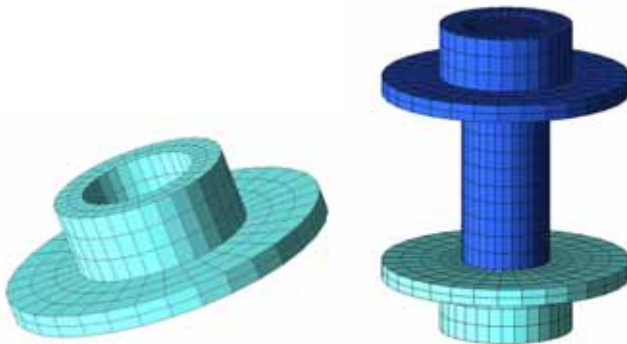


Figure 7. FEA mesh of the nut-washer unit and the fastening units.

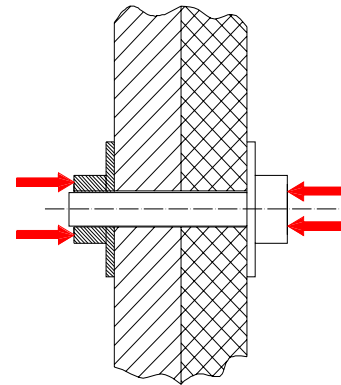


Figure 8. Fastening forces on the joint.

Contacts between the aluminum and epoxy, the aluminum and the steel bolt-washer, the plates and the bolt, and the epoxy and nut-washer were modeled using the contact pair approach in ABAQUS. This approach is based on the master-slave concept, and the contact problem was solved using the Lagrange multiplier method. Since sliding between parts was expected to be small, the “small sliding” option was used in all analyses. This option implied that possible contact between master and slave nodes is defined at the beginning of the analysis and is not redefined during the analysis. The contact surfaces used in the model are shown in Figure 9. Two different surface interaction properties were created for applying two friction coefficients to the contact pairs.

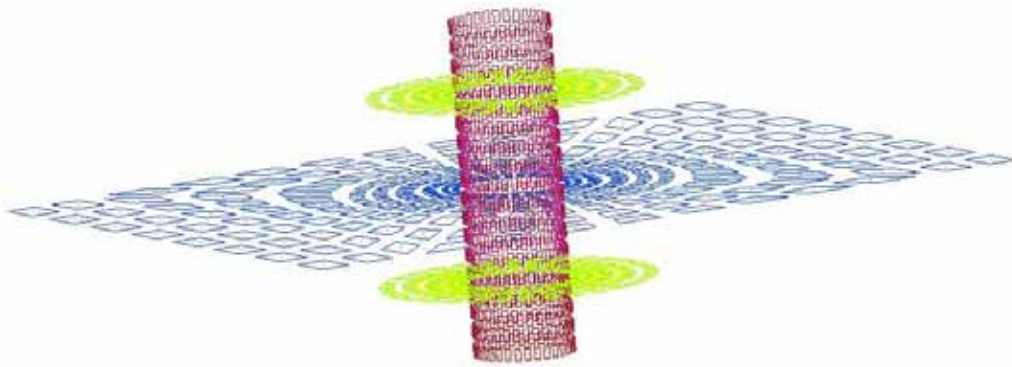


Figure 9. Contact pairs involved in a single lap bolted joint.

The epoxy plate was fixed on one direction at one end. The clamping force was simulated by a distributed nodal load applied on the bolt head and nut in every point of their volume. On the nodes of the end of the aluminum plate, a static force was applied as a distributed load.

RESULTS AND REMARKS

Experimental and numerical results were compared by case.

1. Pin connection

In the first studied case the two plates were connected by a half inch diameter pin. The joint was loaded progressively up to 50lbs. Besides the fringe pattern recorded by the camera, some strain measurement were recorded from inside the tested plate.

The photoelasticity investigation delivered the following result for 50lbs loading on the joint (Figure 10). It can be seen that in the lower left corner, which is the point closest to the aluminum plate during loading, and has the highest shear stress, there are 3.5 fringes (the white lines are full order fringes and the black ones are half order fringes). The Max shear stress is determined as **700 psi**.

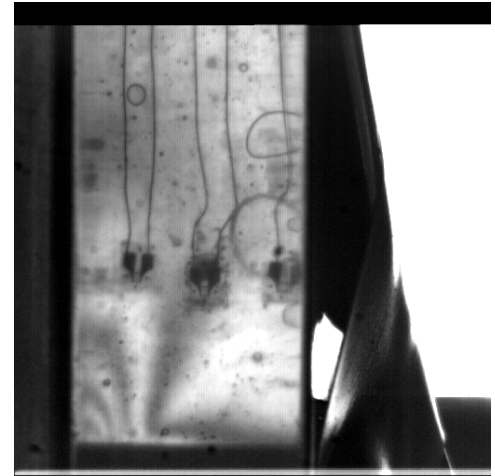


Figure 10. Shear stress fringe pattern for a pin connection loaded at 50lbs.

Figure 11 presents the FEA distribution of the shear stress in the bearing plane (the same as embedded polariscope) and Figure 12 is the distribution of the normal strain in the 2 direction, for 50 lbs load. As it can be seen the map of the shear stress obtained numerically matches the stress distribution pattern obtained by photoelasticity.

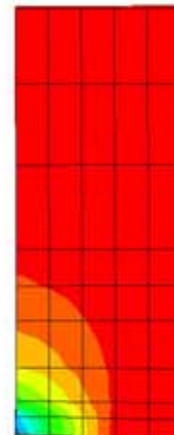
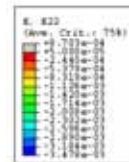
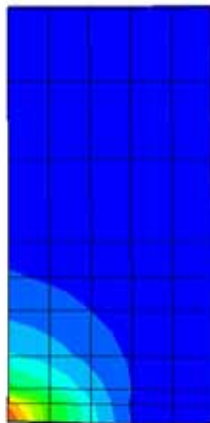
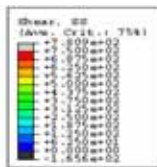


Figure 11. Distribution of shear stresses in the bearing plane of the epoxy plate for pin connection and 50 lbs load on the joint (results are in psi).

Figure 12. Distribution of normal strain in 2-direction in the bearing plane of the epoxy plate (results are in $\mu\epsilon$) for pin connection and 50 lbs load on the joint.

Strain results that were recorded by the strain gages placed in points A, B and C (Figure 13) for different loads as well as shear stress at points D, E, and F from the photoelasticity test are compared in Figures 14 and 15 respectively.

The photoelasticity method used for this experiment, the embedded polariscope, has one major disadvantage. Optical compensation methods cannot be applied in order to obtain an exact value. That is why all the values on the graph have a ± 50 psi error bar.

As can be seen from Figure 15, the numerical results match very closely the experimental ones at points B and C. In point A, the experiment is providing results with higher magnitudes than FEA. Since point A is the closest to the aluminum plate, the cause of the error could be the friction between the two plates, friction that was not accounted for in the numerical model. The maximum stress on the bearing plane is where the epoxy plate meets the aluminum plate and the pin. This is

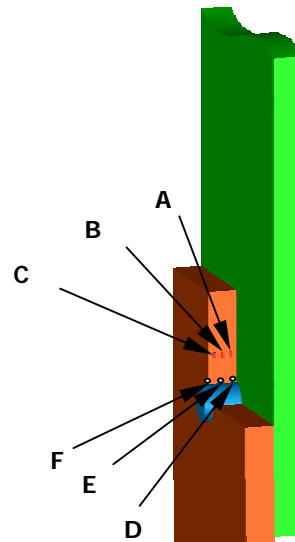


Figure 13. Position of the six measuring points.

the predicted result since the two plates are moving with respect to each other, movement which causes the tilting of the pin. The new position of the pin changes its contact with the plate to a small area. By applying a constraint in the movement of the pin, a decrease in the value of the maximum stress is expected. This constraint can be achieved by replacing the pin with a bolt and applying a torque on the bolt and nut.

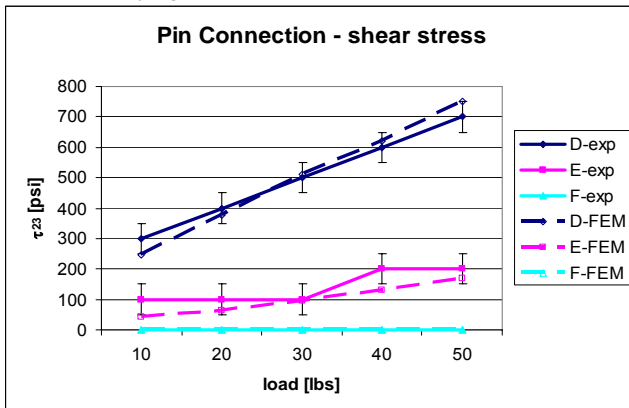


Figure 14. Shear stress in the bearing plane versus the load applied to the joint (pin connected joint).

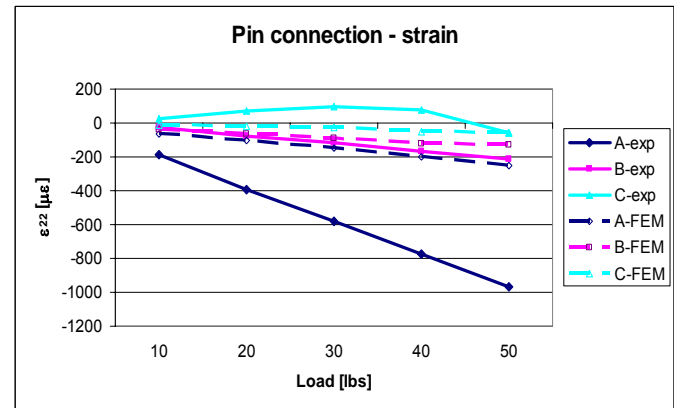


Figure 15. Normal strain in the bearing plane versus the load applied to the joint (pin connected joint).

2. Bolt connection

The pin was replaced by a bolt, on which a torque of about 4 in-lbs was applied, equivalent to finger tightening. The joint was loaded from 0 lbs to 120 lbs. For the maximum load, the shear stress distribution looks like in Figure 16. In Figures 17 and 18, the shear stress results obtained by FEA for 120 lbs load and normal strain for 140 lbs load are presented.

There are no high concentrations of stresses. The distribution is almost uniform. In the left corner there is only one fringe, while on the rest of the lower edge half of a fringe is visible. This means that the highest shear stress is in the same corner as for pin connection; but, for a much higher load, the stress is only about 200 psi. The torque reduces the stress concentration, as expected. Figures 19 and 20 indicate the comparison between test and FEA results.

The difference in stress values obtained by FEA and photoelasticity investigations is under 15 %. That is a reasonable result, taking into consideration that the photoelasticity provides results with a margin of error of 50 psi. As for the pin connection, the strain results are not that close, especially for strain gage number one. The values obtained numerically and experimentally are close for small loads, up to 70 lbs.

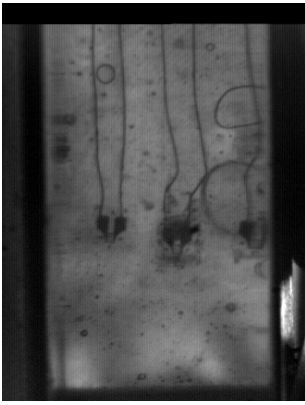


Figure 16. Shear stress fringe pattern for a bolt connection loaded at 50 lbs with a finger tighten.

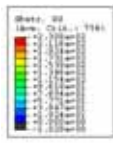


Figure 17. Distribution of shear stresses in the bearing plane of the epoxy plate for 4 in lbs torque on the bolt and 120 lbs load on the joint (results are in psi).

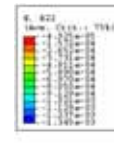


Figure 18. Distribution of normal strain in 2-direction in the bearing plane of the epoxy plate for 4 in lbs torque on the bolt and 140 lbs load on the joint (results are in $\mu\epsilon$).

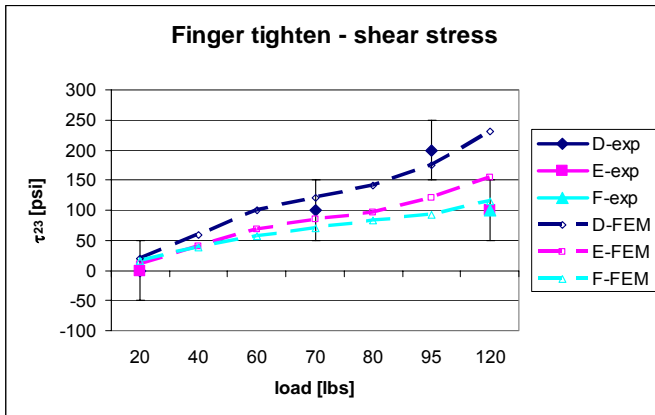


Figure 19. Shear stress in the bearing plane versus the load applied to the joint (bolt connected joint with 4 in lbs torque).

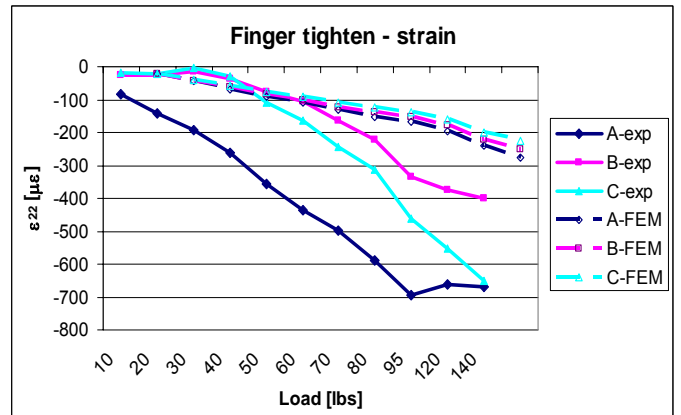


Figure 20. Normal strain in the bearing plane versus the load applied to the joint (bolt connected joint with 4 in lbs torque).

From Figures 10 and 16, two conclusions can be drawn. The magnitudes of stresses are much lower for a bolt connection than for pin connection. That means friction between the two plates is taking over some of the load in the joint. The second conclusion is that the fringe pattern has changed, the stress being more uniformly distributed over the thickness of the plate, which was the desired result.

The bolt was tightened to two different torque levels: 25 in lbs, which was converted to normal loading on the bolt head and nut of 190 lbs. The second torque was 40 in lbs, which was converted to 300 lbs. In Figures 21 and 22, a comparison between the FEA results and the experimental ones is presented for the bolt connection with a torque of 25 in-lbs applied on the bolt. Figure 21 displays the results of the shear stress in the bearing plane, while Figure 22 shows strain values in the same plane.

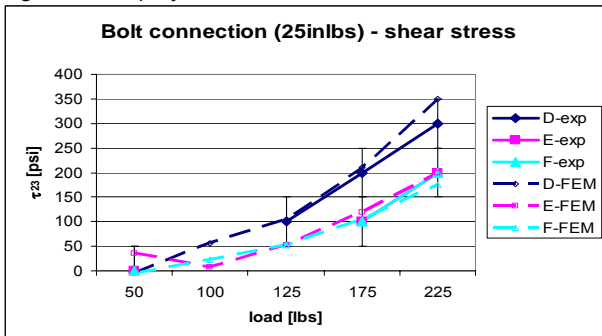


Figure 21. Shear stress in the bearing plane versus the load applied to the joint (bolt connected joint with 25 in-lbs torque).

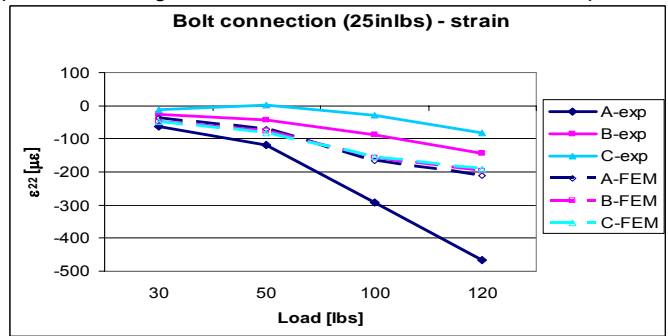


Figure 22. Normal strain in the bearing plane versus the load applied to the joint (bolt connected joint with 25 in-lbs torque).

The shear stresses have very similar values for experimental and numerical results at all three points measured. For the point of maximum stress, FEA predicts a higher value than the experiment, which can only lead to a safety factor in the design of the product.

The strain results provided by experiment and finite element modeling appear to be similar for the middle point only. The causes of errors have both experimental and numerical provenance: delamination of the investigated slice from the plate, which causes false readings from the strain gages, presence of an air bubble next to the third strain gage, and application of the force on the bolt on the same direction through all the steps of the simulation. A more extended discussion about these errors can be founded in section 6.

The same comparisons as for 25 in-lbs torque are displayed in Figures 23 and 24 but for 40 in-lbs torque. As can be seen from Figures 23 and 24, the same remarks as for 25 in-lbs torque can be made (see Figures 21 and 22), which leads to the conclusion that the numerical model provides consistent results.

3. Numerical alternative designs for decreasing the maximum stress

To decrease the stresses in bolted composite plates, two alternative designs were proposed and analyzed numerically. The first design includes a steel bushing around the hole in the plate. A section of the mesh of the plate can be seen in Figure 25. The thickness of the bushing is 0.05 inches and the material has the following properties: $E = 30e6$ psi and $\nu = 0.28$. The role of the bushing is to take over the high stress concentration zone, since steel has a higher ultimate strength. Also, the steel bushing makes the plate stiffer in the longitudinal direction, and especially in the bearing zone.

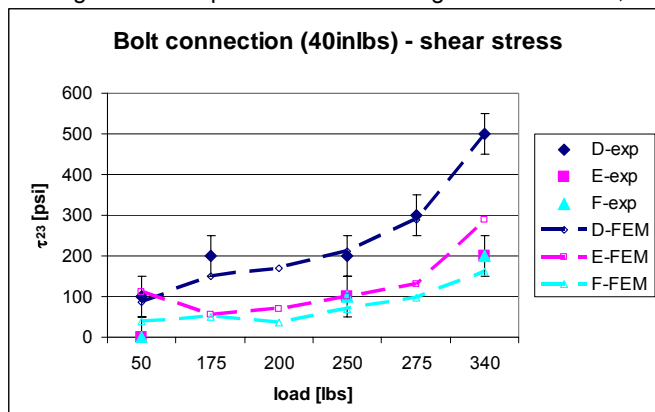


Figure 23. Shear stress in the bearing plane versus the load applied to the joint (bolt connected joint with 40 in-lbs torque).

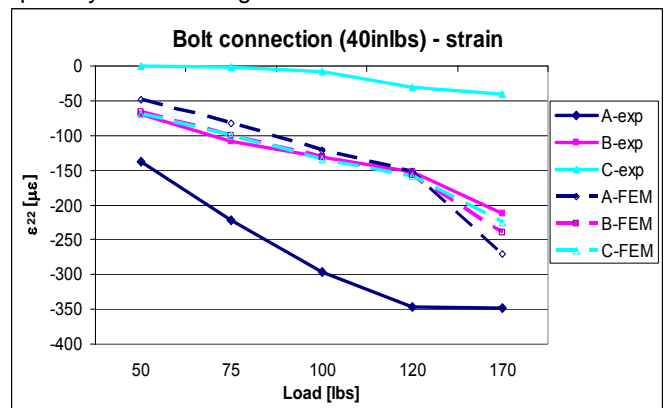


Figure 24. Normal strain in the bearing plane versus the load applied to the joint (bolt connected joint with 40 in lbs torque).

The distribution of the shear stress in the bearing plane for this alternative design can be seen in Figure 26. This load case incorporates 4 in lbs torque on the bolt and 120 lbs loading of the joint.

As can be seen a maximum stress of only 105 psi is developed inside the epoxy plate, while for a regular plate, the stress is 230 psi. This design decreases the maximum stress in the bearing plane of the epoxy plate by 50 %.

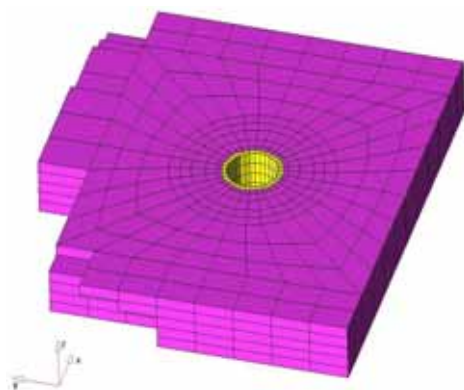


Figure 25. Typical mesh of the plate with a steel bushing around the hole (alternative design one).

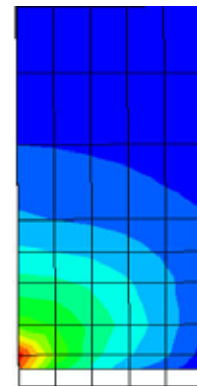
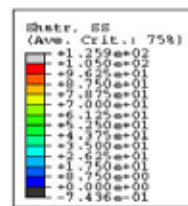


Figure 26. Distribution of shear stresses in the bearing plane of the modified epoxy plate for 4 in lbs torque on the bold and 120 lbs load on the joint (results are in psi).

The second model exhibits a 45 degrees chamfer of the edge of the hole. A portion of the mesh of this alternative design plate can be seen in Figure 27. For this second design the results can be seen in Figure 28. Although the value of the maximum stress has not been lowered, its position has changed. Now, the maximum stress is in the middle of the bearing section, possibly reducing the risk of cracking or, in the laminated composite materials, of delamination.

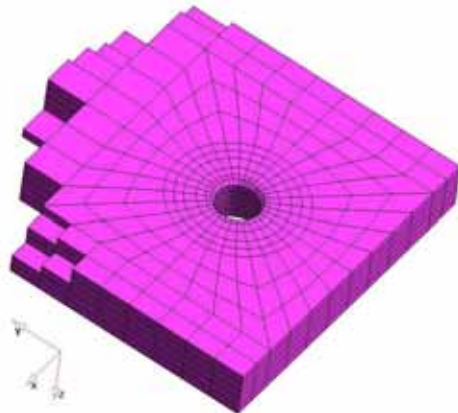


Figure 27. Typical mesh of the plate with a trim of the edge of the hole (alternative design two).

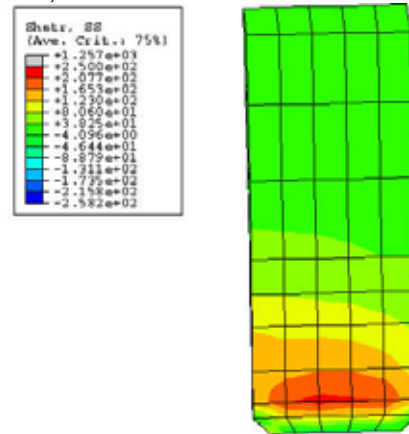


Figure 28. Distribution of shear stresses in the bearing plane of the modified epoxy plate for 4 in lbs torque on the bolt and 120 lbs load on the joint (results are in psi).

DISCUSSION OF RESULTS AND CONCLUSIONS

In this study, several experimental and numerical analyses were conducted to evaluate the behavior of thick single-lap bolted joints. The main interest of this analysis was the stress inside the photoelastic plate along the bearing plane.

Experimental analysis was conducted via photoelastic investigations, by creating an embedded polariscope in the bearing plane of the plate. Additionally, resistance strain gages were mounted inside the plate along the same plane. The numerical modeling was performed with the Abaqus commercial code using material properties and other data obtained experimentally as input. The results were able to explain the behavior of the joint when loaded.

The maximum shear stress in the bearing plane of the photoelastic plate caused by the loading of the joint was created by tilting the bolt. It has been proven that the higher the torque applied on the bolt, the lower the maximum stress in the plate. Yet, if a certain value of this torque is exceeded, failure of the joint will occur. Even a small value of the torque, equivalent with finger tightening the bolt, will decrease the maximum shear stress by more than 50%.

Having confidence in the numerical model created, two other plates were designed in order to decrease the value of the maximum stress. The first plate incorporated a steel bushing around the hole, and the value of the stress in the photoelastic plate was diminished by 50%. The second design presented had the edges of the hole chamfered at a 45 degrees angle. This design didn't show a decrease in the maximum stress, but it showed a change in the position of the maximum stress, to a location less susceptible to cracking or delamination (in the case of laminated composite materials). Taking into consideration that the second design is just a little or no more costly than the original design, it seems to be a good alternative for improving the bolt joining of composite plates, but additional research is needed to prove this contention.

The application of the force on the bolt has to be very closely considered in the future, and a new method has to be found to simulate the torque applied on bolts. If the force is applied to the bolt, this force has to change its orientation together with the orientation of the bolt. Regarding the experiment, an important condition has to be fulfilled: the surfaces of the specimen have to be very smooth, since even the smallest irregularity will create a stress concentration recorded by photoelasticity method.

Future researches will concentrate on applying similar numerical models to complex laminated composite materials. The results will be verified with experiments.

REFERENCES

1. Camanho, P. P. and Matthews, F. L., "Stress analysis and strength prediction of mechanically fastened joints in FRP: a review," *Composites Part A*, 529-547, (1996).
2. Dano, M. L., Gendron, G., et al., "Stress and failure analysis of mechanically fastened joints in composite laminates," *Composite Structures*, 50, 287-296, (2000).

3. Ireman, T., Ranvik, T., et al., "On damage development in mechanically fastened composite laminates," *Composite Structures*, 49, 151-171, (2000).
4. McCarthy, M. A., Lawlor, V. P., et al., "Bolt-hole clearance effects and strength criteria in single-bolt, single-lap, composite joints," *Composite Science and Technology*, 62, 1415-1431, (2002).
5. Park, H. J., "Effects of stacking sequence and clamping force on the bearing strengths of mechanically fastened joints in composite laminates," *Composite Structures*, 53, 213-221, (2001).
6. Starikov, R. and Schon, J., "Quasi-static behaviour of composite joints with protruding-head bolts," *Composite Structures*, 51, 411-425, (2001).
7. Zetterberg, T., Astrom, B. T., et al., "On design of joints between composite profiles for bridge deck applications," *Composite Structures*, 51, 83-91, (2001).
8. Chen, W. H., Lee, S. S. et al., "Three-dimensional contact stress analysis of a composite laminate with bolted joint," *Composite Structures*, 30, 287-297, (1995).
9. Barbero, E. J., Luciano, R., et al., "Three-dimensional plate and contact/friction elements for laminated composite joints," *Computer and Structures*, 54(4), 689-703, (1995).
10. Ireman, T., "Three-dimensional stress analysis of bolted single-lap composite joints," *Composite Structures*, 43, 195-216, (1998).
11. ABAQUS/Standard user manual ver. 6.2. Hibbit, Karlsson & Sorensen, Inc., (1998).
12. HyperMesh user manual ver. 5.0, Altair Computing, Inc., (2001).
13. Speck, J. A., *Mechanical fastening, joining and assembly*, Marcel Dekker, Inc., (1997).